Spin thermoelectric effects in Resonant Tunnelling Diodes

Author
Javier Hernández Nicolau

Supervisor
David Sánchez

Abstract

We consider thermoelectric effects in quantum conductors within the scattering approach. In particular, we study the thermoelectric conductance and Seebeck coeffcient of a Resonant Tunneling Diode (RTD). We obtain a maximum thermopower of the order of k_B/e which shows a conduction of carriers from the hot to the cold reservoir. The maximum can be modified with the position of the energy level in the quantum well E_0 and with the temperature. In the second part of this Master thesis, a spin splitting in the level is included. We find a splitting in the thermopower maximum and the possibility to obtain completely polarized spin currents by modifying the system parameters. Finally, we study the spin thermopower due to the generation of spin biases in response to thermal gradients. Our results show two peaks in the spin thermopower of different sign. This effect involves a spin polarized current for spin-up or spin-down electrons even in the absence of charge current. We discuss optimal values of this effect as a function of temperature.

Resumen

Consideraremos efectos termoeléctricos en conductores cuánticos dentro del formalismo de scattering. En particular, estudiaremos la conductancia termoélectrica y el coeficiente Seebeck de un Diodo Resonante de efecto Túnel. Hemos obtenido un máximo en la termopotencia del orden de k_B/e, el cual muestra una conducción de cargas del reservorio caliente al frío. El máximo puede ser modificiado por la posición del nivel de energía en el pozo cuántico E_0 y por la temperatura. En la segunda parte de este Trabajo de Fin de Master, una división por espín en el nivel es incluida. Encontramos una división en la termopotencia máxima y la posibilidad de obtener corrientes de espín completamente polarizadas modificando los parametros del sistema. Finalmente, estudiamos la termopotencia de espín debida a la aparición de voltajes de espín como respuesta a gradientes térmicos. Nuestros resultados muestran dos picos en la termopotencia de espín. Este efecto involucra una corriente polarizada en espín para los electrones spin-up o spin-down incluso en la ausencia de corriente de carga. Estudiamos valores óptimos de este efecto como función de la temperatura.

Resum

Considerarem efectes termoèlectrics d'espí en conductors quàntics dins el formalisme de scattering. En particular, estudiarem la conductància termoèlectrica i el coeficient Seebeck d'un Diode Ressonant d'efecte Túnel. Hem obtingut un màxim a la termopotència del ordre de k_B/e el qual mostra una conducció de càrregues del reservori calent al fred. El màxim pot esser modificat per la posició del nivell d'energia en el pou quàntic E_0 i per la temperatura. A la segona part d'aquest Treball de Fi de Màster, una divisió per espí en el nivell es inclosa. Trobam una divisió en la termopotència màxima i la possibilitat d'obtenir corrents d'espí completament polaritzades degudes a l'aparició de voltatges d'espí com a resposta a un gradient tèrmic. Els nostres resultats mostren dos pics en la termopotència d'espí. Aquest efecte involucra una corrent polaritzada en espí per electrons spin-up o spin-down fins i tot en abscència de corrent de carrega. Estudiam valors òptims d'aquest efecte com a funció de la temperatura.

Contents

1 Introduction **6**
- 1.1 Nanostructures . . . 6
  - 1.1.1 Semiconductors . . . 7
  - 1.1.2 The Resonant Tunneling Diode (RTD) . . . 7
- 1.2 The Seebeck effect . . . 9

2 Current through the RTD **11**
- 2.1 Formalism . . . 11
- 2.2 Current . . . 12

3 Seebeck effect in a RTD **15**
- 3.1 General formulation . . . 15
- 3.2 Thermoelectric conductance . . . 16
- 3.3 Seebeck coefficient . . . 18

4 Thermoelectric effects in a Magnetic Resonant Tunneling Diode **20**
- 4.1 Currents . . . 21
- 4.2 Spin current and Polarization . . . 23
- 4.3 Thermoelectric conductance . . . 25
- 4.4 Seebeck coefficient . . . 25

5 Spin Seebeck in magnetic RTD **27**
- 5.1 Introduction to the Spin Seebeck effect . . . 27
- 5.2 The Spin Seebeck effect in a magnetic RTD . . . 28

6 Conclusions **31**

A Linearization of the current **32**

B Calculation of the Spin Seebeck effect **34**

Chapter 1

Introduction

1.1 Nanostructures

In the last decades we have seen how the computers (and, in general, the field of the electronics) have improved really fast. It is remarkable how the smartphone you carry in your pocket is much more powerful than the spacecraft which landed in the Moon 40 years ago (which had a RAM of only 1KB). To get better and faster computers, more electronic components are introduced (in particular, more transistors). In 1965 G. Moore, Intel co-funder, predicted that the number of transistors doubled every two years[1]. That law has been fulfilled, at least until now. Nowadays, a common CPU has one billion transistors (for instance, *Intel Core i7*).

In order to get this number of transistors in a practical small computer, the size of transistors have to be reduced. Present technology achieves dimensions of 32nm. The transistors are made of semiconductors, in particular, silicon. In solid silicon, the distance between atoms is 0.2nm, which means that the size of the transistor is approximately 150 atoms. Then, the question is: Can we get transistors as small as we want and apply the "Ohm's law"? For smaller size, the quantum effects can become relevant.

Since the technology for semiconductors allows us to reach these small sizes, we can fabricate structures (what we call *nanostructures* or *mesoscopic systems*) and study their quantum effects. The dimension of nanostructures have the same or similar order of magnitude of present transistors but what has become relevant is their quantum behaviour. The aim of this area is not only the study of the classical concept of current (transport of electrons) but also to use quantum effects to develop new devices with a different behaviour and analyse (and use) new properties as the spin of the electrons. That is, nanostructures do not replace the function of transistors. We study them for academic purposes and their encouraging future applications.

The area of condensed matter that studies the spin properties and their applications to solid state devices is called *Spintronics*. The study of spin and its manipulation is extremely relevant in the development of many future applications, as for example, the quantum computation and the concept of the spin qubit. The advantage of the qubit is that the "classical" bit has only two states (0 and 1), whereas the qubit can be in a superposition of quantum states (namely $\alpha\,|0\rangle + \beta\,|1\rangle$). But there are also existing applications of the spin as, for instance, the Giant Magnetoresistive effect. In this effect, the spin of the electrons in the electron flow is fundamental and with different layers of ferromagnets we can control the current. Discovered in 1988 independently by the groups of A.Fert and P.Grungberg, this effect is broadly used in the present hard drives[2].

In this Master thesis, we have studied the Resonant Tunneling Diode. The choice of that nanostructure is due the fact that no much work have been done in the study of its thermoelectric effects. In addition, it is a nanostructure prototypical which shows quantum effects at temperatures relatively high and it is easy to fabricate.

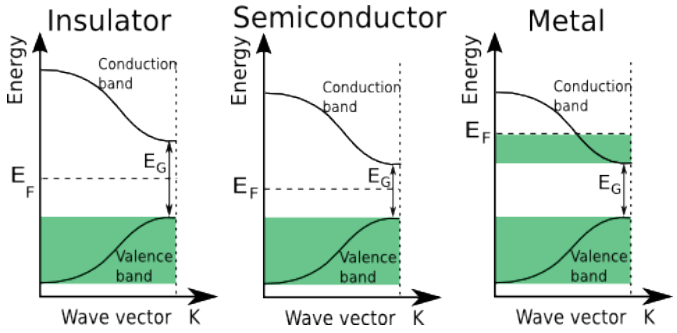

Figure 1.1: **Bands structure.** The insulator and the semiconductor are quite similar, they do not have occupied states in the conduction band. However, the energy gap E_G is bigger in the insulator. For the metal, we have some states occupied in the conduction band.

1.1.1 Semiconductors

We mentioned that the nanostructures can be made of semiconductors. But, what is a semiconductor? An easy answer is that it is a solid material between an insulator and a metal. An insulator is defined as a material with a very high resistivity and the metal is defined as the opposite (very low resistivity). In spite of this, what is more important for us is their band structure. In figure 1.1, the band structure is plotted for the different cases.

The Fermi level E_F indicates the last occupied state allowed (at zero temperature). In all the cases below the Fermi level, if the band allows it, all the states are occupied by electrons. Since there are no allowed energies we say that there is a "gap" between the bands with an energy E_G. In a metal, the Fermi level is in the conduction band and several states are occupied. For the semiconductor and the insulator the E_F is in the gap and no electrons occupy the conduction band at zero temperature.

The difference between the semiconductor and the insulator is that the energy gap E_G is smaller for the semiconductor. In fact, there is no strict definition, but materials with energy gaps lower than 3eV are considered semiconductors. Because of the low energy gap, for non-zero temperature some electrons can be in the conduction band.

Some semiconductors are, for example, Silicon (the most used in semiconductor industry), Germanium and Phosphorous. But there are also compound semiconductors such as GaAs, InSb, ZnSe... Even some carbon allotropes are considered semiconductor as graphene.

The importance in the industry is that the semiconductor can be *doped* with some impurities. The process changes the position of the Fermi level and the density of carriers (electrons or holes). Different doped semiconductors are used in the fabrication of diodes, transistors...

Within band theory and specially in the study of semiconductors, the current can be seen as the flow of electrons in the conduction band or as the flow of holes (absence of electrons) in the valence band. We will focus on the electron flow.

The reason why we use the semiconductors in mesoscopic systems is because the technology to fabricate them is highly developed, their bands structure can be easily modified and we can tune its carrier concentration to a great extent.

1.1.2 The Resonant Tunneling Diode (RTD)

One of the most surprising effects when a student begins to study quantum physics is the tunnel effect. Due the Quantum Mechanics, a free particle can be described as a probabilistic wave function. This wave can penetrate some regions which classically would be impossible. Tunnneling phenomena, for instance, can explain the particle alpha radiation or be used for the Scanning Tunneling Microscope.

In 1973, Leo Esaki was awarded with a Nobel Prize for their experimental discoveries in tunneling phenomena [3]. Part of his work involves the study of the Resonant Tunneling Diode [4] which he discovered in 1958 [5].

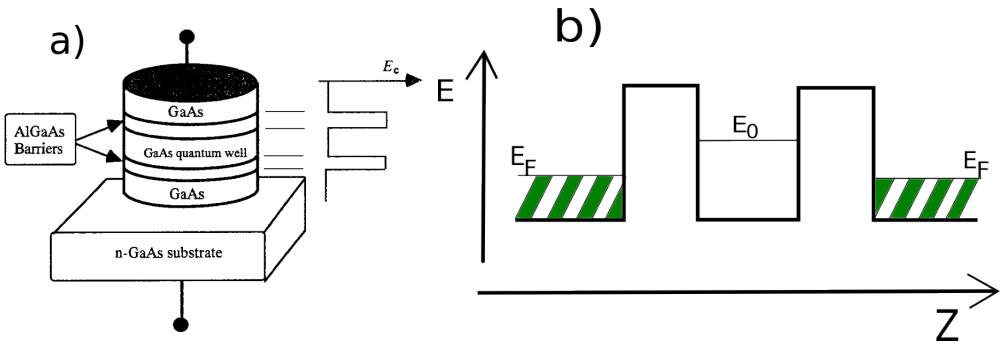

Figure 1.2: **The Resonant Tunneling Diode. (a)**: Layer structure of a real RTD (picture taken from [6]). **(b)**: Schematic view. The E_F is the Fermi level and E_0 is an arbitrary energy level in the potential well.

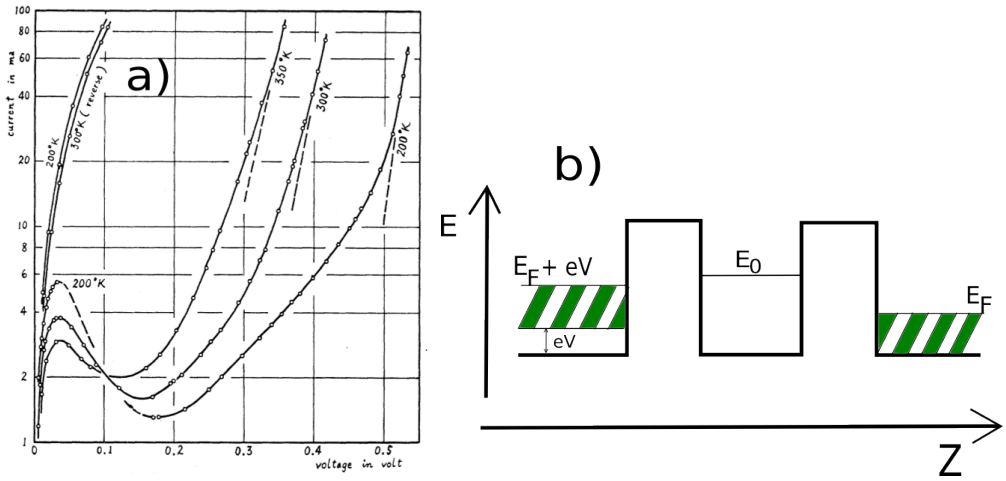

Figure 1.3: **First experimental results of the RTD. (a)**: Esaki's experimental results showing a negative differential resistance [5]. After the drop, the current grows again due the existence of a higher energy level in the well. **(b)**: Schematic of the RTD if a voltage is applied.

The basic idea of the Resonant Tunneling Diode consists of a system where we have two potential barriers that form a potential well between them. In the potential well we have an energy level. Then, a free electron in one side has some probability to tunnel trough one barrier to the allowed level and tunnel again through the second barrier. But, how to implement this in a real system?

In figure 1.2, the experimental setup of a Resonant Tunnelling Diode (RTD) and its schematic is shown. The device is made of different layers of semiconductor. The flow of electrons cross the nanostructure perpendicular to the layers. The barriers are made of a semiconductor with a high energy gap but sufficiently thin for tunnelling. The left and the right side of the RTD are highly doped electronic reservoirs and play the role of the contacts of the nanostructure. In the potential well, we have a discrete energy level. But, we might have more than one or no discrete levels at all.

In absence of electric fields, both electrons from the left and from the right have the same probability to cross the RTD. Therefore, the net current through the system is zero.

However, if we apply a bias an unexpected behaviour will occur. As we increase the voltage one reservoir will have a higher energy and the electrons of this side will have more probability to tunnel. As a result, we will have a current through the Diode. However, for some bias values (the resonance) the current will not longer increase but drop. This effect occurs because the bottom of the band of the the reservoir has passed the energy level E_0, and no electrons can tunnel through the RTD. In figure 1.3 we show the experimental results which Esaki obtained in [5]. Note that some temperatures are close to room temperature.

This strange effect shows that it exists a region where increasing the voltage the current decreases. In

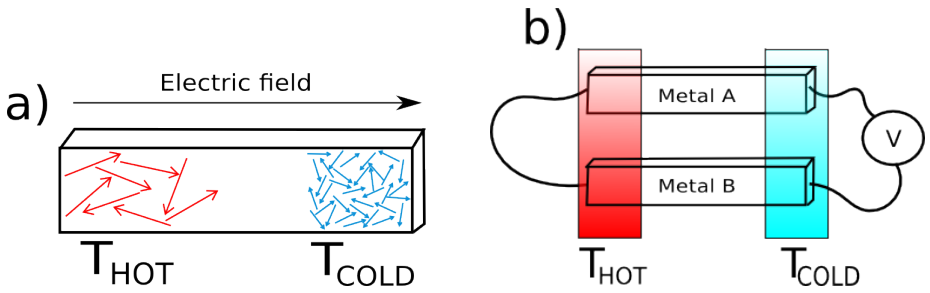

Figure 1.4: **Seebeck effect. (a)**: The hot side has electrons with more velocity than the cold side. For this reason, on average, there are more electrons in the cold side and it creates a bias. **(b)**: Since each material has his own thermopower, if we connect them with a difference in temperature there will be a voltage.

other words, we have a negative differential resistance. For this reason, one of the commercial uses of the RTD is as hight frequency oscillating components.

1.2 The Seebeck effect

In 1821, T.J. Seebeck discovered an interesting effect. Two different metals connected with a temperature difference in the junctions create an electric current trough them (in fact, what Seebeck really observed was a magnetic field). The explanation is easy to understand.

First, we will see what happens in a single metal with a temperature difference, see figure 1.4. The electrons in the hot side have more velocity than in the cold side. Eventually, due to this difference in velocity we will have more electrons in the cold side. Therefore, a bias ΔV has been created and is proportional to the difference in temperature ΔT:

$$\Delta V = S\Delta T \tag{1.1}$$

where S is the Seebeck coefficient(or thermopower) and depends on the material properties. If the carriers that move are electrons, we will have a negative thermopower. But if the carriers are the holes, the thermopwer will be positive.

Then, if we have two different connected materials, we will have a different voltage between them because of the difference in the thermopower. This is the basic idea of Seebeck's discovery which we call *thermocouple*. The thermocouple is broadly used as a thermometer in industry and research. But this is not the only use for the Seebeck effect. Thermoelectrics generators, for instance, can be used to generate electricity from waste energy in a car [7]. Another example is its use in the space: the NASA's Mars *Curiosity* rover uses a thermoelectric generator which uses as a heat source radioactive material [8].

To construct thermoelectric devices, semiconductors are widely used. The reason is the fact that the Seebeck coefficient depends on the electron density and, as we have mentioned before, the semiconductors can be doped to vary their concentration. Consequently, we have a large range of possible values for the S.

Some years after the Seebeck's discover, Peltier observed the opposite behaviour. A difference in voltage creates a difference in temperature. This effect can be used to refrigerate. In fact, today, these devices are used in some refrigerators because they do not have any moving parts or refrigerant. However, they are not efficient enough compared to conventional refrigerators. Similarly, thermoelectric generators are not also very efficient.

The efficiency of a thermoelectric device is directly related to the figure of merit ZT [9]:

$$ZT = \frac{\sigma S^2 T}{\kappa} \tag{1.2}$$

where σ is the electric conductivity and κ is the thermal conductivity which includes the electronic and the lattice (phonons) contributions. To improve the figure of merit the electric conductivity has to be higher and the thermal conductivity lower. But one can notice that these two properties are not easy to be satisfied

at the same time. Higher electric conductivity means more mobility for the electrons but that leads to more thermal conductivity. Focus on the thermopower will be interesting because the figure of merit depends quadratically on it.

In order to have competitive thermoelectric devices in the market we should need $ZT > 3$. However, the best material with higher figure of merit are the alloys of Bi_2Te_3 which has a $ZT \approx 1$ at $T = 300K$ [10]. Many efforts have been done to improve the ZT with little success, in spite of the fact that it does not exist a theoretical limit for the figure of merit.

In the last years, thermoelectrics effects have been studied in nanostructures since in 2001 a $ZT \sim 2.4$ was observed in a superlattice[11]. Confinement of electrons and layered structures can enhance the figure of merit [12][13]. In addition, the low dimensionality can also improve ZT [14][15].

We will focus on the linear response regime:

$$I = G\Delta V + L\Delta T \tag{1.3}$$

where G is the electric conductance and L is the thermoelectric conductance. That is, the current not only depends of a difference in voltage but also a difference in temperature. In the case of an open circuit ($I = 0$) we can relate both conductances to the Seebeck coefficient using equation 1.1:

$$S = \left.\frac{\Delta V}{\Delta T}\right|_{I=0} = -\frac{L}{G} \tag{1.4}$$

Chapter 2

Current through the RTD

2.1 Formalism

In the study of the electron transport in the Resonant Tunnneling Diode we will use the Landauer-Buttiker formalism also know as the scattering approach [16] [17]. The method assumes that elastic scattering exists inside the conductor, namely, the electron does not loss energy in collisions due to impurities. This assumption is valid only for a typical length much smaller than the mean free path in the material. This assumption is quite reasonable for many nanostructures. The scattering approach will give us "simple" expressions as compared to the Green's functions formalism. However, this method does not take into account interactions with impurities (phonons, magnetic impurities...) which in some situations can be relevant. The current will be given by the probability than an electron is transmitted through a nanostructure. In other words, the conductance is a function of the transmission. The model also assumes that the reservoirs are in thermal equilibrium and can be described by the Fermi-Dirac distribution:

$$f_\alpha(E) = \frac{1}{1 + e^{(E-\mu_\alpha)/k_B T_\alpha}} \tag{2.1}$$

where α is the terminal index, k_B is the Boltzmann constant, T_α is the temperature of terminal α and μ_α is its electrochemical potential (which takes into account the energy due to the voltage bias eV):

$$\mu_\alpha = E_F + eV_\alpha \tag{2.2}$$

In addition, the current through our two terminal nanostructure in the Landauer-Buttiker formalism can be expressed in general by:

$$I = 2\frac{e}{h}\sum_n \int T_n(\mathbf{E})\left[f_L(\mathbf{E}) - f_R(\mathbf{E})\right] d\mathbf{E} \tag{2.3}$$

where e is the charge of the electron, h is the Planck constant, the sum over n is the sum over the n different transmission channels(that is, states with the same energy), $\mathbf{E}$ the energy of the carriers and $T_n(\mathbf{E})$ is the transmission function.

The demonstration of eq 2.3 is rather long (see ref.[16] for a full demonstration), but we can see qualitatively that it makes sense because the current has to be proportional to the probability to have an occupied state in the left reservoir times to have an unoccupied one in the right reservoir minus the probability to have an occupied in the right one times to have an unoccupied in the left one. Mathematically this is:

$$I \propto f_L(1 - f_R) - f_R(1 - f_L) = f_L - f_R \tag{2.4}$$

The equation 2.3 is quite general for different nanostructures. Actually, what makes the difference for different devices is the transmission function. This contains the information of how the electron is scattered. In the case of a RTD, we have assumed that we have one (or more) discrete energy level in the quantum

well. For an infinite quantum potential well this is true, but in our physical system the barriers have a finite height and electrons can tunnel through them.

The transmission can be obtained numerically solving the Schrödinger equation of the system. Quite generally, the transmission shows resonant peaks who can be approximated by a Lorentzian function:

$$T(E) = \frac{\Gamma_L \Gamma_R}{(E - E_0)^2 + \left(\frac{\Gamma_L + \Gamma_R}{2}\right)^2} \tag{2.5}$$

where E_0 is the center (and our energy level value in the potential well) and the parameters Γ_L (Γ_R) are modelled as the rates with which an electron between the barriers can leak out through the left barrier (right barrier). This is is the so-called Breit-Wigner approximation[18].

2.2 Current

In a junction of two different semiconductors, reservoir and barrier respectively, due the highly doped reservoir we have a two-dimensional electron gas (2-DEG). This effect creates a layer (in the junction) where the electrons behave effectively as free electrons with an effective mass m^*. As a result, energy subbands are created with energy:

$$\mathbf{E} = E_z + E_\perp = E_z + \frac{\hbar^2}{2m^*}\left(k_x^2 + k_y^2\right) \tag{2.6}$$

As in the introduction, we consider z as the direction perpendicular to the layers ($x-y$ plane) and k is the wave number of each direction.

In eq. 2.3 we can perform the sum over the states. We can consider the sum in the continuous limit and with the density of states of a two dimensional system $D_{2D}(E)$

$$D_{2D}(E) = \frac{Am}{2\pi\hbar^2} \tag{2.7}$$

we obtain:

$$I = \frac{em^*A}{2\pi^2\hbar^3} \int T\left(\mathbf{E}\right)\left[f_L\left(\mathbf{E}\right) - f_R\left(\mathbf{E}\right)\right] d\mathbf{E} \tag{2.8}$$

where A is the area of the device.

Our system is invariant in the plane perpendicular to z direction, as well as the current we calculate. Consequently, the transmission will only depend on the energy along the Z direction:

$$I = \frac{em^*A}{2\pi^2\hbar^3} \int_{eV}^{\infty} dE_z\ T\left(E_z\right) \int_0^{\infty} dE_\perp [f_L\left(E_\perp + E_z\right) - f_R\left(E_\perp + E_z\right)] \tag{2.9}$$

The limits of the integral take all the possible values of energy, whereas in the z direction the allowed energy begins from the bottom of the band (which we redefine as our zero). However, if a voltage is applied, the bottom of the band shifts an energy eV as we can see in figure 1.3.

The integrals of the Fermi-Dirac distribution are:

$$\int_0^{\infty} dE_\perp\ \frac{1}{1 + e^{(E_\perp + E_z - \mu)/k_B T}} = k_B T \ln\left[1 + e^{-(E_z - \mu)/k_B T}\right] \tag{2.10}$$

Therefore, the current will be:

$$I = \frac{em^*A}{2\pi^2\hbar^3} k_B T \int_{eV}^{\infty} dE_z\ T\left(E_z\right) \ln\left[\frac{1 + e^{-(E_z - \mu_L)/k_B T}}{1 + e^{-(E_z - \mu_R)/k_B T}}\right] \tag{2.11}$$

The expression 2.11 is called the *Esaki formula* [19]. The term:

$$k_B T \ln\left[\frac{1+e^{-(E_z-\mu_L)/k_BT}}{1+e^{-(E_z-\mu_R)/k_BT}}\right] \tag{2.12}$$

is known as the *supply function* because it determines the relative weight of available carriers at a given perpendicular energy. The behaviour of this function is similar to the Fermi-Dirac distribution. For small temperatures it can be described as a step function (in fact it is not a completely step function, because the vertical step has a slope which begins in the E_F and finishes in $E_F + eV$). But for higher temperatures the "step" becomes smoother.

To study the current we will need to substitute the expression of the transmission (eq. 2.5). To make the current dimensionless we define:

$$I_0 = \frac{2\pi\Gamma_L\Gamma_R}{\Gamma}\frac{e}{h} \tag{2.13}$$

where $\Gamma = \Gamma_L + \Gamma_R$. In this thesis we use equal barriers with the same tunneling rate, consequently, $\Gamma_L = \Gamma_R = \frac{\Gamma}{2}$. Typically, the Γ is of the order of $1 - 10\ meV$ [20]. Therefore:

$$I_0 \sim 10^{-6} = 1\mu A \tag{2.14}$$

As a result, the normalized current is:

$$\frac{I}{I_0} = \frac{m^* A}{2\pi^2\hbar^2} k_B T \int_{eV}^{\infty} dE_z \ \frac{\Gamma}{(E-E_0)^2 + \left(\frac{\Gamma}{2}\right)^2} \ln\left[\frac{1+e^{-(E_z-\mu_L)/k_BT}}{1+e^{-(E_z-\mu_R)/k_BT}}\right] \tag{2.15}$$

In order to represent this function, we will need to give some values to the parameters because we have to represent I numerically. In each figure of the Master thesis, the used parameters will be specified except the effective mass of the electron and the area of the diode. Although our model is theoretical, we will use parameters from real experiments. For the effective mass we set:

$$m^* = 0.03 m_e \tag{2.16}$$

The value corresponds to the ZnSe, where m_e is the mass of the electron. For example, other typical values of the effective mass are $0.067 m_e$(GaAs) and $0.013 m_e$(InSb).

We will use an area of the device from a real experiment, for instance in [20]:

$$A = 100\mu m^2 \tag{2.17}$$

Note this value is much higher if we compare with the width of the layers. For instance, in [20], the barriers have a width of only $10nm$.

In figure 2.1, we can see the current calculated from our theoretical model. We have a maximum when the bottom of the band has the same energy as the E_0. However, if we compare with the experimental result in figure 1.3, we do not have the smooth decay after the maximum (the small tail we have theoretical is due the Lorentzian shape). The reason is mainly due to the inelastic scattering and phonons present in the device [16] [20] [21] and our scattering model neglects them. One should notice that we do not have also the second current growth after the drop. That is because this *growth* is due to the second level in the potential well. And in our theoretical model we do not take into account. Note that it can be included just modifying the transmission function.

Nevertheless, the model describes the physics of the device. If we apply a bias, the electrons in one reservoir have more probability to jump through the device. We can increase the voltage and more electrons can tunnel until we reach a bias for which the bottom of the band is aligned with the energy level of the well. At that moment, we have the maximum. For a higher bias all the electrons have more energy and the electron flow drops. Notice the effect of temperature, a higher temperature means more energy for the electrons and for small bias they have more probability to jump (compared with "colder" electrons) which gives us a higher value of current.

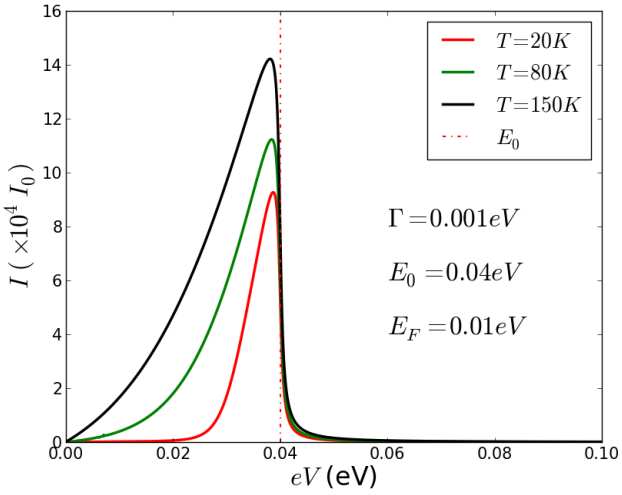

Figure 2.1: **Theoretical current.** The current shows a maximum when the bottom of the band reaches the energy level of the well E_0 (dashed line). For higher temperatures the current has a high value even for low values of bias. The reason is that for high temperatures the electrons have more energy and, consequently, more probability to jump.

Chapter 3

Seebeck effect in a RTD

3.1 General formulation

In this section, we will focus on the effects of a temperature difference applied along the contacts of our RTD. We have a reference temperature T. But, in our system, we will have two different temperatures T_L and T_R for the left and right reservoir respectively. The notation used is $T_L = T + \theta_L$ and $T_R = T + \theta_R$ where the θ are small temperature differences. Then:

$$\Delta T = T_L - T_R = (\theta_L - \theta_R) \tag{3.1}$$

Using the same formalism as in the previous section(eq. 2.9), we can obtain the current in the case of a temperature difference:

$$I = \frac{em^*A}{2\pi^2\hbar^3} k_B \int_{eV}^{\infty} dE_z \; T(E_z) \left[T_L \ln\left(1 + e^{-(E_z-\mu_L)/k_B T_L}\right) - T_R \ln\left(1 + e^{-(E_z-\mu_R)/k_B T_R}\right)\right] \tag{3.2}$$

To obtain the Seebeck coefficient and study the thermoelectric effects at linear response, one should linearize the above expression in to the form of eq. 1.3:

$$I = GV + L\Delta T \tag{3.3}$$

The steps to obtain the next expression are included in appendix A. Thence, the current can be written as:

$$I = \frac{em^*A}{2\pi^2\hbar^3} k_B \int_{eV}^{\infty} dE_z \; T(E_z) \times \left(\frac{1}{k_B} f_{FD}(E_z)\, eV \right.$$
$$\left. + \Delta T \left[\frac{E_z - E_F}{k_B T} \; f_{FD}(E_z) + \ln\left(1 + e^{-(E_z-E_F)/k_B T}\right)\right]\right) \tag{3.4}$$

Therefore, we can identify G and L:

$$G = \frac{e^2 m^*A}{2\pi^2\hbar^3} k_B \int dE_z \; T(E_z) \left[\frac{1}{k_B} f_{FD}(E_z)\right] \tag{3.5}$$

$$L = \frac{em^*A}{2\pi^2\hbar^3} k_B \int dE_z \; T(E_z) \left[\frac{E_z - E_F}{k_B T} \; f_{FD}(E_z) + \ln\left(1 + e^{-(E_z-E_F)/k_B T}\right)\right] \tag{3.6}$$

Finally, we can write a general expression for the Seebeck coefficient as defined in equation 1.4 for $I = 0$:

$$S = \frac{V}{\Delta T} = -\frac{k_B}{e} \frac{\int dE_z \; T(E_z) \left[\frac{E_z - E_F}{k_B T} \; f_{FD}(E_z) + \ln\left(1 + e^{-(E_z-E_F)/k_B T}\right)\right]}{\int dE_z \; T(E_z) \left[f_{FD}(E_z)\right]} \tag{3.7}$$

Notice this is valid for any possible transmission. However, to study these expressions we will use the Lorentzian transmission (eq. 2.5).

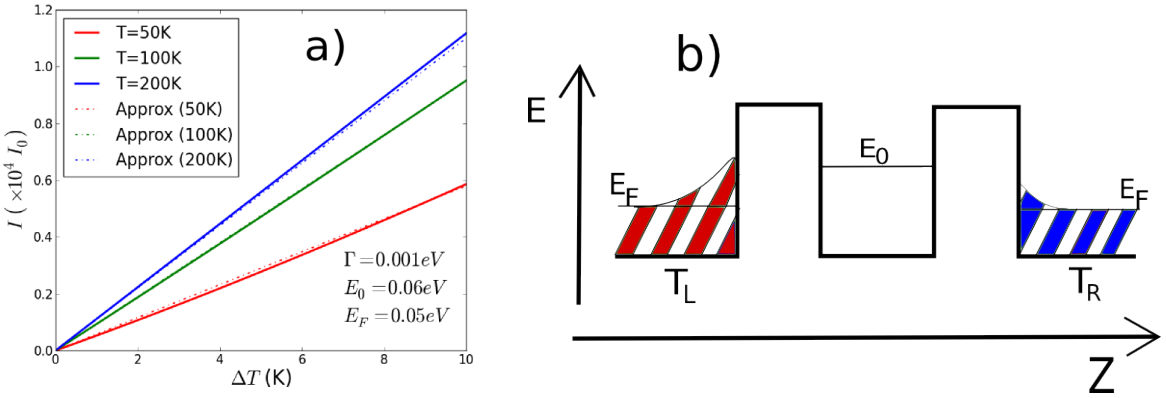

Figure 3.1: **Current for a temperature difference ΔT. (a)**: The solid lines are the current using the general equation. The dashed lines represent the charge flow using the linear approximation. Notice that the approximation is good for $T >> \Delta T$. **(b)**: Schematic of the RTD for two different temperatures.

3.2 Thermoelectric conductance

Now, we will assume no applied voltage and only a difference in temperature. With the approximation done in the previous section, we have the carrier flow written in the form:

$$I = L\ \Delta T \tag{3.8}$$

We now discuss the validity of our linear-response theory. In the figure 3.1, we plot the current using the general equation (3.2) in solid lines and in dashed lines we represent the current using our approximation:

$$I/I_0 = \tilde{L}\ \Delta T \tag{3.9}$$

where the thermoelectric conductance $\tilde{L}$ is:

$$\tilde{L} = \frac{m^* A}{4\pi^2\hbar^2} k_B \int dE_z\ \frac{\Gamma}{(E_z - E_0)^2 + \left(\frac{\Gamma}{2}\right)^2} \left[\frac{E_z - E_F}{k_B T}\ f_{FD}\left(E_z\right) + \ln\left(1 + e^{-(E_z - E_F)/k_B T}\right)\right] \tag{3.10}$$

We find that the approximation is quite good for $T >> \Delta T$, as should be as one can notice in figure 3.1 because solid and dashed lines are quite indistinguishable.

We have observed a current which is due completely to a temperature difference. The electrons have more energy in the hot side and have more probability to jump through the device. Note that a high temperature difference will be difficult to obtain in a mesoscopic system and for this reason we will have small values of current if we compare with current by applied bias (see figure 2.1).

Now, we will study the thermoelectric conductance. In figure 3.2 $\tilde{L}$ is plotted as a function of the position of the energy level of the quantum well. Notice that the function reaches a maximum when the position of the energy level E_0 is the same as the Fermi energy level of the reservoirs. In other words, if we have the same value for E_0 and E_F, we will have a maximum of $\tilde{L}$ and also for the current with no applied voltage bias.

This behaviour is unexpected. One should expect that for E_0 higher than Fermi level we have conduction of electrons and consequently a positive $\tilde{L}$. At the same time, for $E_0 < E_F$ one should expect a conduction with holes and a $\tilde{L} < 0$. Recently, in experiments with quantum dots this situation has been observed[22]. However, in our case, the $\tilde{L}$ is always positive and with a maximum in $E_0 = E_F$. That means that we always have conduction from the hot reservoir to the cold one.

A possible answer to this behaviour is found in the supply function. As in the previous chapter, we can define a supply function from eq. 3.2. Then:

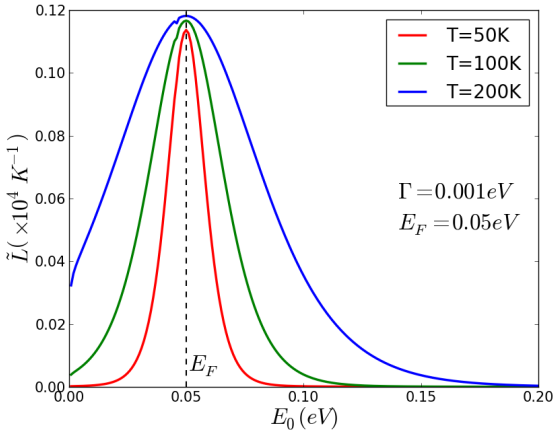

Figure 3.2: **Thermoelectric conductance by the position of the E_0 level in the RTD.** The function is centered in E_F (where the maximum is) and for different temperatures the width changes as a linear function, $FWHM \simeq 4k_BT$. Notice that the function is always positive which implies that the conduction of carriers is always from the hot to the cold reservoir.

$$k_B \left[T_L \ln\left(1 + e^{-(E_z-\mu_L)/k_B T_L}\right) - T_R \ln\left(1 + e^{-(E_z-\mu_R)/k_B T_R}\right)\right] \tag{3.11}$$

is the supply function for a temperature difference in a RTD.

If we focus on a temperature difference with no applied voltage, that is

$$\mu_L = \mu_R = E_F \tag{3.12}$$

we find that the supply function behaves exactly as L. It is always positive and has a maximum in $E_z = E_0 = E_F$ which implies that the maximum of available carriers occurs at $E_0 = E_F$.

In addition, we can study the width of the $\tilde{L}$ and its dependence with the temperature. We have made numerical simulations to obtain the Full Width at Half Maximum (FWHM) and, for the parameters used, we have obtained the relation:

$$\text{FWHM}_{\tilde{L}} \approx 4k_BT \tag{3.13}$$

The expression for $\tilde{L}$ (eq.3.10) does not have a fully analytical result. All the calculations are made numerically. However, it will be interesting to have an analytical result. One possible solution will be to approximate the Lorentzian to a delta function centered in E_0:

$$T\left(E_z\right) = 2\pi \frac{\Gamma_L \Gamma_R}{\Gamma} \delta\left(E_z - E_0\right) \tag{3.14}$$

In the figure 3.3, there are two plots. The left one is our function $\tilde{L}$ for different Γ except the dashed line which is for the approximation of a delta function. Notice for small Γ the delta approximation is quite good. In the right plot of figure 3.3, the maximum of the $\tilde{L}$ has been plotted for different values of Γ. It can be seen that for $\Gamma < 10meV$ the approximation to a delta is enough good. Recent work in RTD, as in [20], shows a $\Gamma \sim 10meV$.

We previously found that the $\tilde{L}$ has a maximum for $E_0 = E_F$. Using the approximation of the delta function we can find the maximum of the function $\tilde{L}$ easily by making a derivative which, as expected, gives us a maximum if:

$$E_0 = E_F \tag{3.15}$$

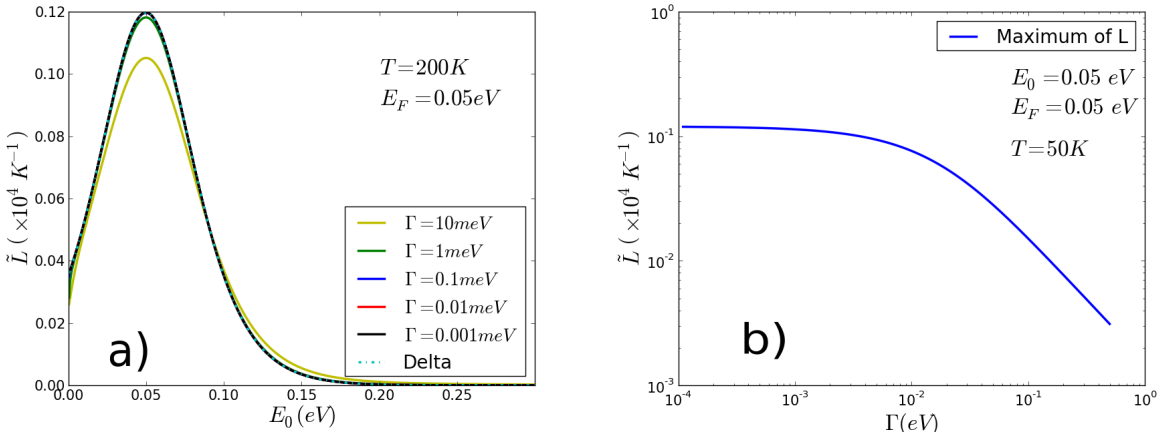

Figure 3.3: **Influence of Γ in $\tilde{L}$. (a)**: It shows the $\tilde{L}$ for different Γ. **(b)**: it represents the maximum of $\tilde{L}$ in a logarithmic scale, showing that for $\Gamma < 10meV$, the approximation to a delta is good enough.

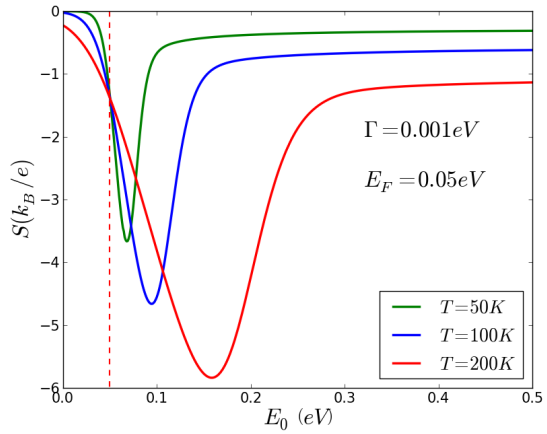

Figure 3.4: **Seebeck coefficient.** The thermopower has a maximum (in absolute value) which shifts for higher temperatures. The dashed line indicates the position of the Fermi level.

3.3 Seebeck coefficient

Using the Lorentzian transmission and the Seebeck expression calculated in equation 3.7 we obtain for the RTD:

$$S = -\frac{k_B}{e}\frac{\int dE_z \ \frac{\Gamma}{(E_z-E_0)^2+\left(\frac{\Gamma}{2}\right)^2}\left[\frac{E_z-E_F}{k_BT}\ f_{FD}\left(E_z\right)+\ln\left(1+e^{-(E_z-E_F)/k_BT}\right)\right]}{\int dE_z \ \frac{\Gamma}{(E_z-E_0)^2+\left(\frac{\Gamma}{2}\right)^2}\left[f_{FD}\left(E_z\right)\right]} \tag{3.16}$$

As one can see, the Seebeck coefficient(or thermopower) is independent of the area of the RTD and the effective electron mass. The function only depends on the parameters Γ and E_F of our device.

The S is represented in figure 3.4. The thermopower is always negative for any value of the position of the energy level in the quantum well. This is completely related to the issue discussed before in the $\tilde{L}$. We always have conduction of the carriers from the hot reservoir to the cold one.

One can compare the results with the experiments done with quantum dots[22]. It was found that a thermovoltage V_T ($V_T = -S\Delta T$) was generated due the presence of a temperature difference. The sign of this voltage can change with the position of the energy level of the quantum dot. If the position of the energy level is above or below the Fermi level we will have a different sign of V_T. That means a conduction of

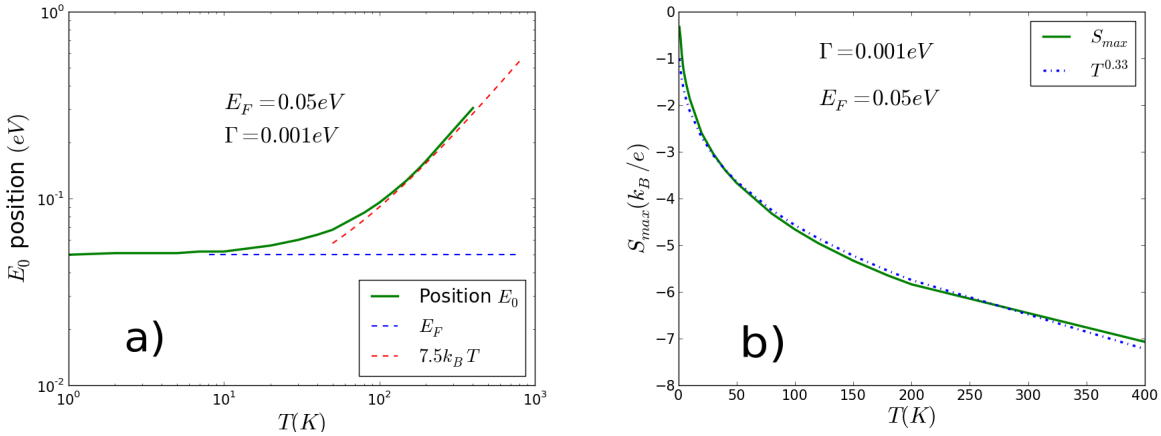

Figure 3.5: **Position and maximum value of the thermopower.** The left picture represents the position of the maximum value of S in logarithmic scale. It suggests that for small temperatures the position of the maximum is at $E_0 = E_F$ but for $T > O\left(10^2\right)$ the position change as linear function of temperature. For the right picture, it can be observed the maximum (in absolute value) of the Seebeck coefficient is a function of temperature changing as a power function.

holes or electrons depending of the energy level of the quantum dot. However, this behaviour is not present in our Resonant Tunneling Diode.

In addition, although $\tilde{L}$ has a maximum in E_F independently of temperature, in the case of the Seebeck coefficient its minimum (maximum in absolute value) does depend on T. In the figure 3.5, we can see how the position where the minimum occurs changes as:

$$E_0 = \begin{cases} E_F, & \text{if } T < O\left(10^1\right) K \\ \approx 7.5 k_B T, & \text{if } T > O\left(10^2\right) K \end{cases} \tag{3.17}$$

In other words, for small temperatures the minimum value occurs at E_F, but for higher ones the position changes as a linear function of temperature.

Moreover, we can study how the minimum value of S is modified with the external temperature T. In figure 3.5 one can see that this value depends on temperature as:

$$|S|_{\max} \propto T^{0.33} \tag{3.18}$$

As we have done before for the $\tilde{L}$, we can calculate the width of the thermopower function and observe its dependence. Its width also follows a linear expression:

$$\text{FWHM}_S \approx 8.6 k_B T \tag{3.19}$$

which is consistent with the dependence of the width in thermoelectric conductance (see eq. 3.13).

Our results demonstrate that the Seebeck coefficient in a RTD can be manipulated with the external temperature T and with the position of the quantum well level E_0.

Chapter 4

Thermoelectric effects in a Magnetic Resonant Tunneling Diode

In order to add spin effects in our device, we have to introduce the concept of diluted magnetic semiconductor (DMS). In a DMS, magnetic ions are added to a semiconductor with the purpose of having a ferromagnetic behaviour. In the absence of magnetic field, its behaviour is similar to a regular semiconductor, whereas in the presence of a magnetic field, it shows a splitting in the energy levels higher than the Zeeman effect. For this reason, this effect is called the *giant Zeeman effect*[24].

The (normal) Zeeman effect produces that degenerate angular momentum quantum states are split because of a magnetic field. In general, each state has its magnetic dipole moment associated with it and, as a result, the splitting is different. Both, the orbital and spin moments are involved in this effect. Furthermore, the displacement from the degeneracy ΔE can be written as:

$$\Delta E = g_L \mu_B m_j B \tag{4.1}$$

where g_L is the electron Landé g-factor (describes the magnitude of the effect and depends of the spin-orbit interaction), μ_B is the Bohr magneton, m_j is the z component of the total angular momentum and B is the magnetic field.

However, in dilute magnetic semiconductors, a strong exchange interaction occurs between the d-electrons of the magnetic atoms and the band electrons. The giant Zeeman effect is produced by the influence of the net alignment in the free carriers. The energy splitting can be described by a Brillouin function [21] [23]:

$$\Delta E = N_0 \alpha x s_0 B_s \left[s g \mu_B B / k_B \left(T + T_{\text{eff}} \right) \right] \tag{4.2}$$

where $N_0\alpha$ is the exchange integral, x is the diluted magnetic material concentration, s the magnetic material spin and B_s is the Brillouin function. s_0 and T_{eff} are the effective spin and the effective temperature respectively which are phenomenological parameters.

For the normal Zeeman effect the splitting is of the order of $0.1 \sim 0.01 meV$, but for the giant Zeeman effect the splitting can be of the order of $1 \sim 10 meV$ [25].

In this chapter, we will study the thermoelectric effects in a RTD but with a magnetic material in the potential well (see fig. 4.1), that is, a diluted magnetic semiconductor. The characteristic $I - V$ of this nanostructure has been studied, for instance, in [23]. However, thermoelectric effects have not been analysed yet.

Due to the presence of a magnetic field, as we have seen, the energy level of the well splits because the giant Zeeman effect and becomes two levels $E_{0\uparrow}$ and $E_{0\downarrow}$ which label the spin up and spin down levels. They can be written as:

$$\begin{array}{rcl} E_{0\uparrow} & = & E_O + \frac{h}{2} \\ E_{0\downarrow} & = & E_O - \frac{h}{2} \end{array} \tag{4.3}$$

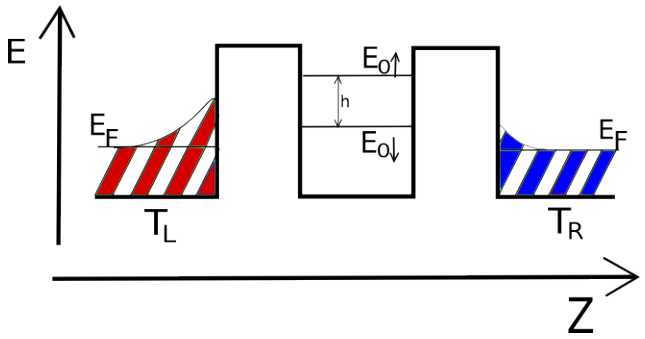

Figure 4.1: **Magnetic Resonant Tunneling Diode.** The schematic view shows a splitting h of the energy level in the potential well due the giant Zeeman effect. Each level only allows current for spin-up or spin-down electrons.

h (or ΔE) is the separation of the energies and can be controlled with a magnetic field B as we have seen in eq. 4.2.

4.1 Currents

If we want to calculate the total carrier flowing through the magnetic RTD we should take into account that we have two contributions, the current of spin up and for the spin down electrons, $I_\uparrow$ and $I_\downarrow$ respectively. Therefore:

$$I = I_\uparrow + I_\downarrow \tag{4.4}$$

The expression for the currents will be quite similar to the non-magnetic RTD (eq. 3.2) but we have a factor 1/2 due the to spin and the transmission functions are correspondingly centered in the energy level of their spin. Consequently:

$$I_\uparrow = \frac{em^*A}{4\pi^2\hbar^3}k_B\int dE_z\ \frac{\Gamma_L\Gamma_R}{(E-E_{0\uparrow})^2+\left(\frac{\Gamma_L+\Gamma_R}{2}\right)^2}\left[T_L\ln\left(1+e^{-(E_z-\mu_L)/k_BT_L}\right)-T_R\ln\left(1+e^{-(E_z-\mu_R)/k_BT_R}\right)\right] \tag{4.5}$$

$$I_\downarrow = \frac{em^*A}{4\pi^2\hbar^3}k_B\int dE_z\ \frac{\Gamma_L\Gamma_R}{(E-E_{0\downarrow})^2+\left(\frac{\Gamma_L+\Gamma_R}{2}\right)^2}\left[T_L\ln\left(1+e^{-(E_z-\mu_L)/k_BT_L}\right)-T_R\ln\left(1+e^{-(E_z-\mu_R)/k_BT_R}\right)\right] \tag{4.6}$$

Similarly as in the previous section, we linearize the expressions above to study the linear response regime:

$$\begin{aligned} I_\uparrow &= L_\uparrow\Delta T + G_\uparrow V \\ I_\downarrow &= L_\downarrow\Delta T + G_\downarrow V \end{aligned} \tag{4.7}$$

After some calculations (quite similar to appendix A) we obtain:

$$I_\uparrow = \frac{em^*A}{4\pi^2\hbar^3}k_B\int_{eV}^{\infty}dE_z\ \frac{\Gamma_L\Gamma_R}{(E-E_{0\uparrow})^2+\left(\frac{\Gamma_L+\Gamma_R}{2}\right)^2}\times\left(\frac{1}{k_B}f_{FD}\left(E_z\right)eV\right.$$
$$\left.+\Delta T\left[\frac{E_z-E_F}{k_BT}\ f_{FD}\left(E_z\right)+\ln\left(1+e^{-(E_z-E_F)/k_BT}\right)\right]\right) \tag{4.8}$$

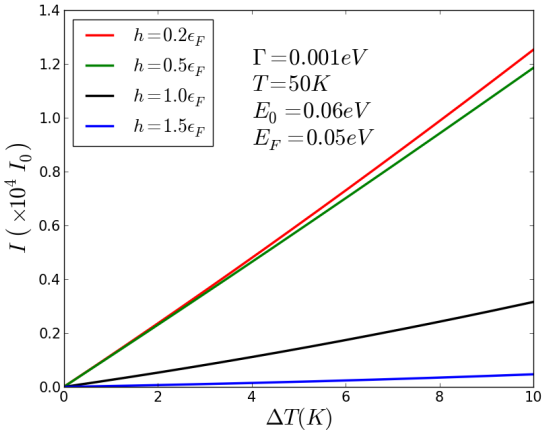

Figure 4.2: **Linearized current for the magnetic RTD.** As we increase the difference in temperature (ΔT), the current also increases. But if we increase the splitting h the intensity decreases.

$$I_\downarrow = \frac{em^*A}{4\pi^2\hbar^3}k_B\int_{eV}^{\infty}dE_z\ \frac{\Gamma_L\Gamma_R}{(E-E_{0\downarrow})^2+\left(\frac{\Gamma_L+\Gamma_R}{2}\right)^2}\times\left(\frac{1}{k_B}f_{FD}\left(E_z\right)eV\right.$$
$$\left.+\Delta T\left[\frac{E_z-E_F}{k_BT}\ f_{FD}\left(E_z\right)+\ln\left(1+e^{-(E_z-E_F)/k_BT}\right)\right]\right) \quad (4.9)$$

Therefore, we can identify the electric and thermoelectric conductances as :

$$G_\uparrow = \frac{em^*A}{4\pi^2\hbar^3}k_B\int_{eV}^{\infty}dE_z\ \frac{\Gamma_L\Gamma_R}{(E-E_{0\uparrow})^2+\left(\frac{\Gamma_L+\Gamma_R}{2}\right)^2}\frac{1}{k_B}f_{FD}\left(E_z\right)e \quad (4.10)$$

$$G_\downarrow = \frac{em^*A}{4\pi^2\hbar^3}k_B\int_{eV}^{\infty}dE_z\ \frac{\Gamma_L\Gamma_R}{(E-E_{0\downarrow})^2+\left(\frac{\Gamma_L+\Gamma_R}{2}\right)^2}\frac{1}{k_B}f_{FD}\left(E_z\right)e \quad (4.11)$$

$$L_\uparrow = \frac{em^*A}{4\pi^2\hbar^3}k_B\int_{eV}^{\infty}dE_z\ \frac{\Gamma_L\Gamma_R}{(E-E_{0\uparrow})^2+\left(\frac{\Gamma_L+\Gamma_R}{2}\right)^2}\left[\frac{E_z-E_F}{k_BT}\ f_{FD}\left(E_z\right)+\ln\left(1+e^{-(E_z-E_F)/k_BT}\right)\right] \quad (4.12)$$

$$L_\downarrow = \frac{em^*A}{4\pi^2\hbar^3}k_B\int_{eV}^{\infty}dE_z\ \frac{\Gamma_L\Gamma_R}{(E-E_{0\downarrow})^2+\left(\frac{\Gamma_L+\Gamma_R}{2}\right)^2}\left[\frac{E_z-E_F}{k_BT}\ f_{FD}\left(E_z\right)+\ln\left(1+e^{-(E_z-E_F)/k_BT}\right)\right] \quad (4.13)$$

Notice now that these transport coefficients become spin-dependent.
As before, we analyse the current for a temperature difference ΔT written in the form:

$$I/I_0 = \left(\tilde{L}_\uparrow+\tilde{L}_\downarrow\right)\Delta T \quad (4.14)$$

In the figure 4.2, we show the total linearised intensity as a function of ΔT, for different splittings h. As one can expect, current increases with increasing temperature difference. In spite of that, if we increase h the intensity will decrease. The reason is the position of the splitted levels. For higher h the $E_{0\uparrow}$ increases and the electrons need more temperature to reach it. At the same time the $E_{0\downarrow}$ decreases and for energies below the Fermi level the current drops as we will see.

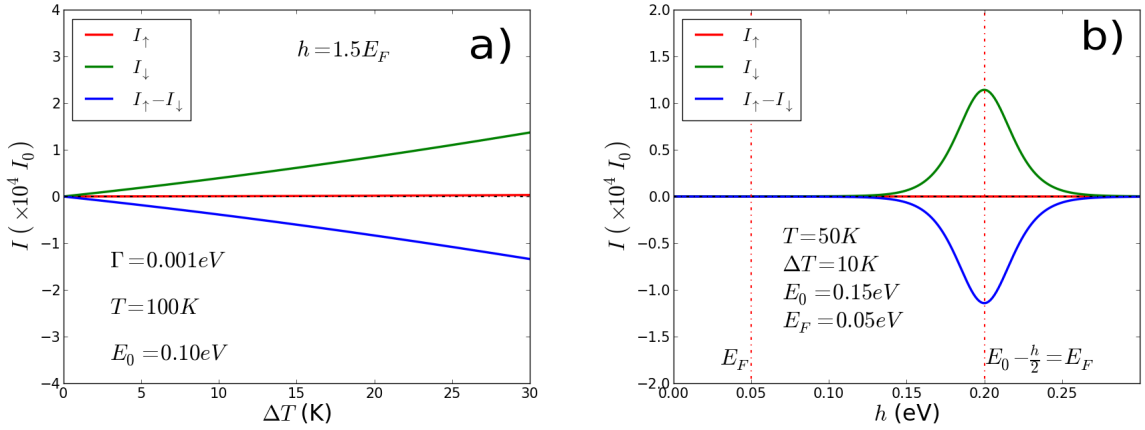

Figure 4.3: **Spin current. (a)**: The current increasess with the temperature difference. The spin down current dominates. **(b)**: The spin down intensity has a maximum (as the spin current) when the splitting is $E_0 - \frac{h}{2} = E_F$. The peak occurs when the spin down level $E_{0\downarrow}$ has the same energy as the Fermi level.

4.2 Spin current and Polarization

Another interesting point will be to study the spin current in our device for possible future applications in spintronics. The total spin current is:

$$I_S = I_\uparrow - I_\downarrow \tag{4.15}$$

In figure 4.3, the spin current is plotted. In the left picture, one can see the currents for each spin. Both increase if the temperature difference is increased. Spin-up current $I_\uparrow$ is smaller due to the parameters we have set. In this section we try to explain the reason for these very low values. In the right picture, we can observe that the $I_\downarrow$ has a maximum (and the total spin current has a minimum) when:

$$E_0 - \frac{h}{2} = E_F \tag{4.16}$$

but the $I_\uparrow$ (too small to be visible in the plot) decays with h. The reason of this peak is, as in the previous chapter, related to the behaviour of $\tilde{L}$. The peak occurs when the spin-down level $E_{0\downarrow}$ reaches the Fermi level (E_F).

Notice that in the right picture, the h axis finishes at 0.3. We cannot go beyond that value because:

$$E_0 - \frac{h}{2} = 0 \tag{4.17}$$

In other words, the spin down level has reached the bottom of the band.

The peak in the spin current has similar properties as the peak in $\tilde{L}$ in the previous chapter (as one should expect since the peak is due the behaviour of the thermoelectric conductance $\tilde{L}$). A temperature change of the external temperature T makes the peak becomes wider. If we change the position of E_0 the peak shifts accordingly.

In figure 4.4 the total spin current is shown for different values of ΔT. For small temperature difference, the spin current is lower. This behaviour agrees with our previous discussion: if we have small temperature difference, the carrier flow will be smaller.

We have observed that, for our parameters, the dominant current is the spin-down current. Then, is it possible a case where the dominant current is due the spin-up level? Yes, it is possible and it depends on the position of the energy level in the potential well as we will see.

For clarity, we introduce the concept of spin polarization. Since we have a current through the RTD it will be useful to define the degree of polarization (that is, what kind of spin current is predominant). The definition of spin polarization P is defined in terms of I_S and the total current I:

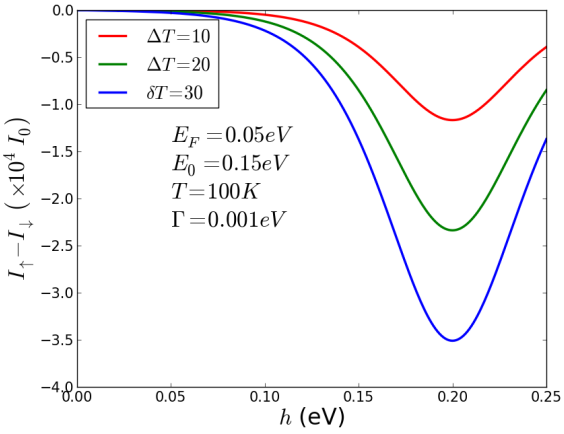

Figure 4.4: **Spin current for different** ΔT. If the temperature difference increases the spin current will also increase.

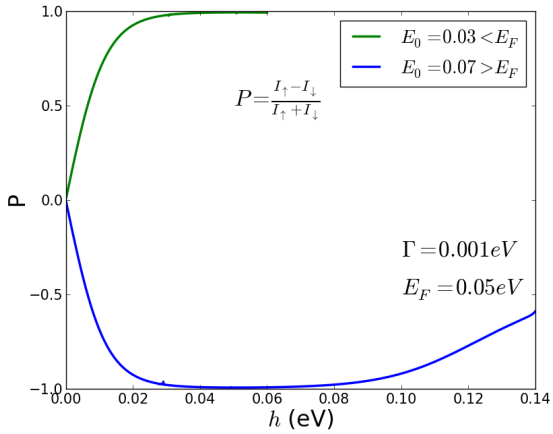

Figure 4.5: **Polarization of the current**. The plot shows the spin polarization of the current as a function of h. The sign of the polarization depends on the position of the E_0 in the quantum well. The positive P function has to finish on $h = 0.06eV$ where the $E_{0\downarrow}$ reaches the zero value.

$$P = \frac{I_\uparrow - I_\downarrow}{I_\uparrow + I_\downarrow} \tag{4.18}$$

In the figure 4.5 the polarization has been plotted. For high values of h the current is completely polarized (1 or -1) for a given spin direction. As one can see, the sign of the polarization depends on the position of E_0.

Therefore, to have a polarization in spin-up, we need to have E_0 below the E_F. This is because in this case, the level which reaches the Fermi level as we increase h will be $E_{0\uparrow}$. On the other hand, we will have spin-down polarization if the E_0 is above the Fermi level, because for some h the $E_{0\downarrow}$ will reach E_F. To sum up:

$$P \begin{cases} \leq 0 & \text{if } E_0 > E_F \\ \geq 0 & \text{if } E_0 < E_F \end{cases} \tag{4.19}$$

Nevertheless, a case where different signs in polarization exist for a fixed E_0 and a variable h is not possible. However, we have shown that a fully polarized spin current can be induced by a temperature

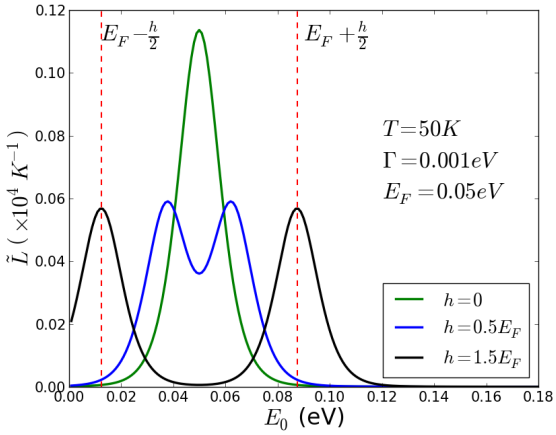

Figure 4.6: $L = L_\uparrow + L_\downarrow$. The peak splits in two maxima in the presence of h. The splitting becomes visible when h is greater than the FWHM. The dashed lines correspond to the position of the maxima at $h = 1.5E_F$

difference in our device and the sign (spin-up or spin-down) can be controlled by the position of the energy level in the quantum well E_0.

4.3 Thermoelectric conductance

We can analyse L which can be defined from equation 4.14 as:

$$\tilde{L} = \tilde{L}_\uparrow + \tilde{L}_\downarrow \tag{4.20}$$

In figure 4.6 we can see how $\tilde{L}$ changes for different h. The peak splits and it appears two new maxima. The position of these maxima is at:

$$E_0 = E_F \pm \frac{h}{2} \tag{4.21}$$

which confirms that the maximum occurs when the splitted energy levels $E_{0\uparrow}$ or $E_{0\downarrow}$ reach the Fermi level E_F. That is, the maxima occur when the splitting levels have the same energy as the Fermi level. The splitting turns to be relevant for:

$$h \sim \text{FWHM} \tag{4.22}$$

Regarding the previous section, we can state that the left and the right peaks have predominant current spin up and spin down respectively. Then:

$$\begin{array}{rcl} I_\uparrow \text{ max} & \rightarrow & E_0 = E_F - \frac{h}{2} \\ I_\downarrow \text{ max} & \rightarrow & E_0 = E_F + \frac{h}{2} \end{array} \tag{4.23}$$

In conclusion, we have found that if we aim at generating spin polarized current, we can tune the position of the energy level E_0 in the quantum well and the applied magnetic field (which modifies h). In fact, for specific parameters we obtain full spin polarization.

4.4 Seebeck coefficient

The thermopower S for a (normal) Resonant Tunneling Diode always shows a negative peak whose minimum depends on the position of the energy level in the quantum well and also on temperature. In this section we will study the effect of the splitted states in S.

From equation 4.7 we can write the total current as:

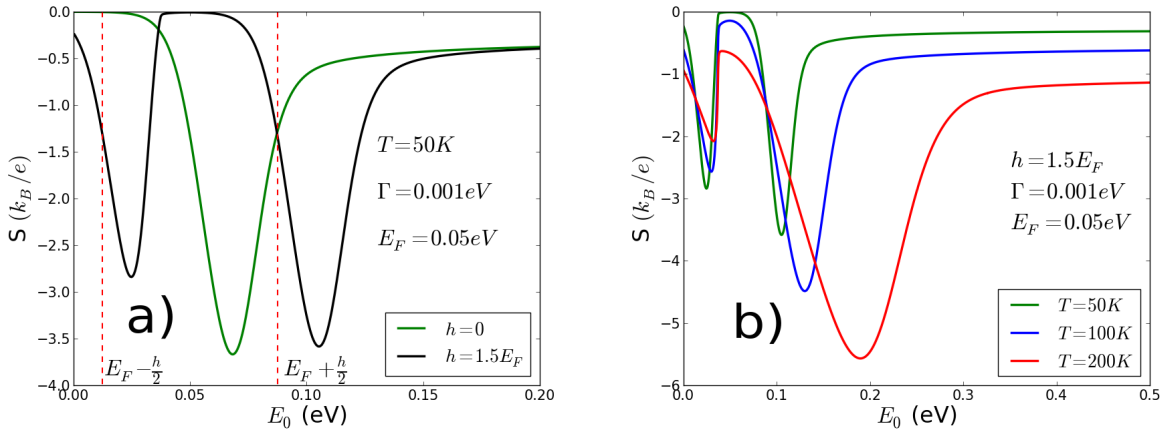

Figure 4.7: **Thermopower for a magnetic RTD**. **(a)**: Thermopower with and without magnetic field (h). Two peaks appear in the splitting case with a small shift from the two spin energy states. **(b)**: For a constant h and different temperatures. One of the peaks increases with temperature but the other one becomes smaller.

$$I = I_\uparrow + I_\downarrow = (L_\uparrow + L_\downarrow)\,\Delta T + (G_\uparrow + G_\downarrow)\,V \tag{4.24}$$

Therefore, the Seebeck coefficient can be written as:

$$S = -\frac{L_\uparrow + L_\downarrow}{G_\uparrow + G_\downarrow} \tag{4.25}$$

In figure 4.7, the thermopower is plotted. In the left picture, we can see that the magnetic field produces a splitting in the Seebeck coefficient and, as one can expect, the position is quite close to the splitted energy levels.

In the right picture the magnetic field is constant and we change the temperature. This increase in temperature implies that one of the peaks increases and the other one decreases. However, for small temperatures, both minima have the same height.

In the previous chapter (no presence of magnetic field) we had showed that the Seebeck coefficient was always negative suggesting that the charge transport is always from the hot to the cold contact. Now, due the influence of the magnetic field, we have obtained a thermopower also negative but with a splitting. Therefore, the inclusion of splitting energy levels does not affect the charge transport from the hot to the cold reservoir.

We have shown that in order to obtain the maximum efficiency in the Seebeck coefficient, we can modify the position of E_0 to choose the higher value of S which also depends of the external temperature T.

Chapter 5

Spin Seebeck in magnetic RTD

5.1 Introduction to the Spin Seebeck effect

In general, the electrochemical potential μ in the presence of a electric potential is defined as:

$$\mu = E_F + eV \tag{5.1}$$

In fact, in solid-state physics, the voltage is defined as the difference of electrochemical potentials of two leads.

However, we can have different electrochemical potentials $\mu_\uparrow$ and $\mu_\downarrow$ for each spin-up and spin-down electrons respectively due to, for example, a spin accumulation[26]. It can occur when the spin diffusion time is short. We will define the mean electrochemical potential of an arbitrary contact α as:

$$\mu_\alpha = \frac{1}{2}\left(\mu_{\alpha\uparrow} + \mu_{\alpha\downarrow}\right) \tag{5.2}$$

The difference $\mu_\uparrow - \mu_\downarrow$ can be seen as a spin electric potential. Therefore, we can define a *spin voltage* as the difference of spin electric potential between two contacts:

$$eV_S = (\mu_{\uparrow L} - \mu_{\downarrow L}) - (\mu_{\uparrow R} - \mu_{\downarrow R}) \tag{5.3}$$

This spin voltage can drive a spin current through the sample. We can have spin-polarized current even in a case where no potential is applied, in other words, in a case with no electrical current. See figure 5.1.

As a consequence, one can ask if the conventional idea of the thermoelectric effect can be applied to the case of a spin voltage. This is, can a difference in temperature create a spin voltage? This phenomenon is called the spin Seebeck effect and has been studied theoretically (for instance [27]) and experimentally [28].

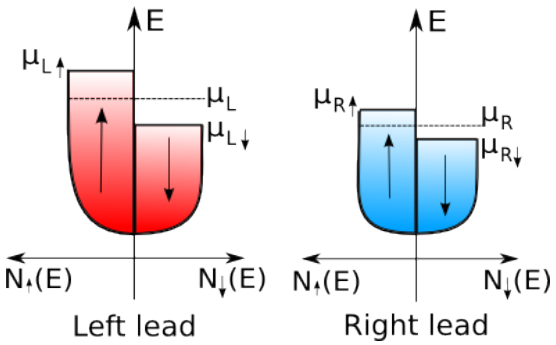

Figure 5.1: **Schematic of the density of states $N(E)$.** In a general case, we have two leads with different temperatures and the electrochemical potentials for spin are different. Notice that in an arbitrary case where $\mu_L = \mu_R$ (not shown in the picture) we can have spin voltage (which produces spin current) but no total electric current.

Since the spin thermopower S_S is the possibility to create a spin voltage by a temperature difference, we can define:

$$S_S = -\left.\frac{eV_S}{\Delta T}\right|_{I=I_S=0} \tag{5.4}$$

The main purpose to study the effect is to use temperature difference to obtain completely spin polarized currents which are essential in spintronics devices. For instance, they could be used as thermoelectrical spin injectors. In addition, this effect does not involve a (normal) current through the device which leads to dissipation and heat.

5.2 The Spin Seebeck effect in a magnetic RTD

The spin Seebeck effect has been studied in quantum dots[27] and metallic samples[28]. Here, we will study the effect in a magnetic RTD (see figure 4.1). In equation 1.3 we show the linearization of the current for the parameters ΔT and eV. But now, we can include the spin voltage eV_S. As a result, the current and the spin current can be written as:

$$I = I_\uparrow + I_\downarrow = (L_\uparrow + L_\downarrow)\,\Delta T + (G_\uparrow + G_\downarrow)\,eV + \frac{1}{2}(G_\uparrow - G_\downarrow)\,eV_S \tag{5.5}$$

$$I_S = I_\uparrow - I_\downarrow = (L_\uparrow - L_\downarrow)\,\Delta T + (G_\uparrow - G_\downarrow)\,eV + \frac{1}{2}(G_\uparrow + G_\downarrow)\,eV_S \tag{5.6}$$

In the appendix B we include the calculations to obtain these expressions and the spin-dependent transport coefficients for our magnetic RTD:

$$G_\uparrow = \frac{em^*A}{4\pi^2\hbar^3}\int_{eV}^{\infty} dE_z\ \frac{\Gamma_L\Gamma_R}{(E-E_{0\uparrow})^2 + \left(\frac{\Gamma_L+\Gamma_R}{2}\right)^2}\left[\frac{1}{k_B}\frac{1}{1+e^{(E_z-E_F)/k_BT}}\right] \tag{5.7}$$

$$G_\downarrow = \frac{em^*A}{4\pi^2\hbar^3}\int_{eV}^{\infty} dE_z\ \frac{\Gamma_L\Gamma_R}{(E-E_{0\downarrow})^2 + \left(\frac{\Gamma_L+\Gamma_R}{2}\right)^2}\left[\frac{1}{k_B}\frac{1}{1+e^{(E_z-E_F)/k_BT}}\right] \tag{5.8}$$

$$L_\uparrow = \frac{em^*A}{4\pi^2\hbar^3}\int_{eV}^{\infty} dE_z\ \frac{\Gamma_L\Gamma_R}{(E-E_{0\uparrow})^2 + \left(\frac{\Gamma_L+\Gamma_R}{2}\right)^2}\left[\frac{E_z-E_F}{k_BT}\ \frac{1}{1+e^{(E_z-E_F)/k_BT}} + \ln\left(1+e^{-(E_z-E_F)/k_BT}\right)\right] \tag{5.9}$$

$$L_\downarrow = \frac{em^*A}{4\pi^2\hbar^3}\int_{eV}^{\infty} dE_z\ \frac{\Gamma_L\Gamma_R}{(E-E_{0\downarrow})^2 + \left(\frac{\Gamma_L+\Gamma_R}{2}\right)^2}\left[\frac{E_z-E_F}{k_BT}\ \frac{1}{1+e^{(E_z-E_F)/k_BT}} + \ln\left(1+e^{-(E_z-E_F)/k_BT}\right)\right] \tag{5.10}$$

Note that the coefficients are the same as the obtained in the magnetic RTD chapter. Nevertheless, a new term in the charge current appears in the linearized charge current. In the same way, we have an expression for the linear response in the spin current I_S in terms of the electric and thermoelectric conductances.

With the condition of zero charge current and zero spin current, the spin thermopower of our diode is then:

$$S_S = -\left.\frac{eV_S}{\Delta T}\right|_{I=I_S=0} = \left(\frac{L_\uparrow}{G_\uparrow} - \frac{L_\downarrow}{G_\downarrow}\right) \tag{5.11}$$

It is important to notice that we have to apply a bias in order to have zero current (total and spin):

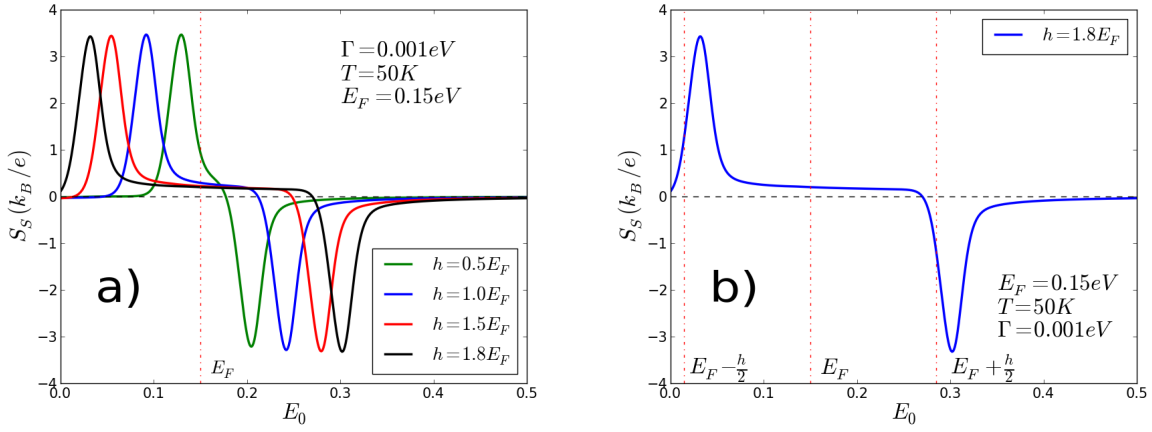

Figure 5.2: **Spin Seebeck coefficient. (a)**: we have the spin thermopower for different splittings in the energy levels. **(b)**: we can see that the position of the peaks versus splitting level represented by the dashed lines. Note that in the spin Seebeck coefficient we have positive and negative values in contrast with the charge thermopower studied in previous chapters.

$$eV = -\frac{\Delta T}{2}\left(\frac{L_\uparrow}{G_\uparrow} + \frac{L_\downarrow}{G_\downarrow}\right) \tag{5.12}$$

In the figure 5.2, we plot the Spin Seebeck coefficient for different magnetic field (different h) in the quantum well. The behaviour is similar to the charge thermopower but now, we have two peaks with different signs. We recall that in the spinless case in the RTD we always obtained a negative thermopower which implies the same charge transport process in the sample (from hot to cold side). Similarly, in the presence of a magnetic field the magnetic RTD shows two peaks but the values of the coefficients are also always negative, that is, the same charge transport. However, here we have obtained different sign in the spin thermopower. Therefore, we can have a spin bias due to a temperature difference:

$$eV_S = -S_S \Delta T \tag{5.13}$$

and this bias can change its sign if we modify the position of the energy level. Consequently, we can also have different signs of spin currents from temperature differences applied to RTDs.

If we look carefully to the equation 5.11 this result can be expected. This expression can be seen as a sum of two Seebeck coefficients for two different energy levels but with opposite signs:

$$S_S = -\left.\frac{eV_S}{\Delta T}\right|_{I=I_S=0} = \left(\frac{L_\uparrow}{G_\uparrow} - \frac{L_\downarrow}{G_\downarrow}\right) \approx S_\uparrow - S_\downarrow \tag{5.14}$$

The position of the peaks are close to the splitting levels as one can see in the right picture of figure 5.2. This behaviour is similar to the obtained in the study of the (normal) Seebeck effect in the magnetic RTD.

In addition, we will study the effect of the temperature in the spin thermopower. The temperature influence is showed in figure 5.3. The peaks size and width of the S_S change with temperature as one can see in the left picture. We can study the effect of temperature in the maxima(in absolute value) of the peaks (see right picture). Here, the spin Seebeck coefficient have two maxima (in absolute value) for some value of temperature (for the parameters used in the plot, close to $50K$). For very low and high temperatures the spin thermopower goes to zero. In comparison, we had found for a non magnetic RTD that the maximum thermopower is a function of T ($T^{0.33}$). Nevertheless, the spin thermopower is not a monotonic function of temperature as the charge thermopower and shows a maximum.

The results obtained here show that we can find different signs of the spin thermopower which implies different signs in the spin bias due to a temperature difference ΔT. This spin bias can produce a spin

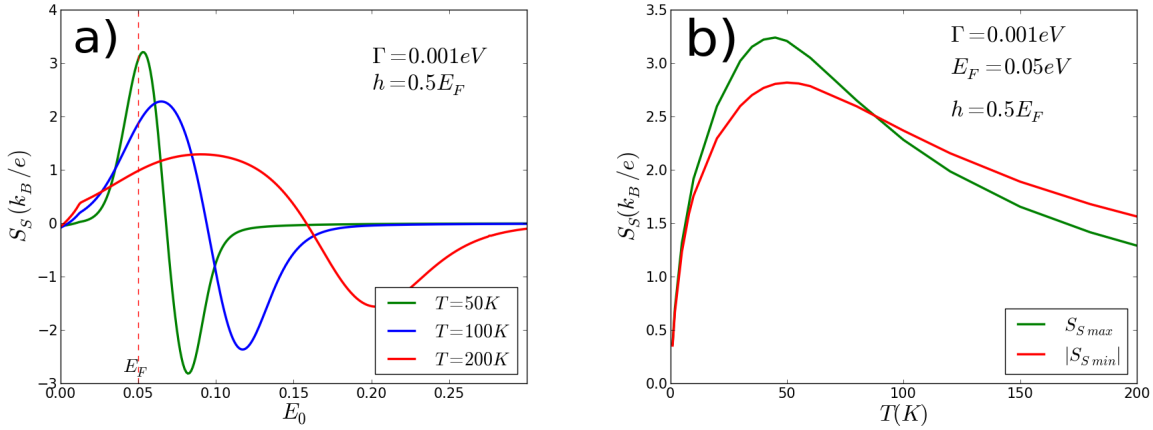

Figure 5.3: **Influence of the temperature in the spin Seebeck effect. (a)**: we have showed the spin thermopower for different temperatures. **(b)**: we have plotted the maxima of the spin thermopower versus temperature. It shows that the spin thermopower has maxima for some values of temperature.

current. Hence, we can obtain different spin current from a temperature difference by varying the position of E_0 in the device. In addition, this effect can be maximally enhanced for some value of E_0 at specific values of the magnetic field. Furthermore, the effect has a maximum for a specific value of temperature.

Chapter 6

Conclusions

In this Master thesis, we have studied the thermoelectric effects in the magnetic (and non-magnetic) RTD. We have observed that modifying some parameters as the position of the energy level, the magnetic field or the temperature, we can obtain high values of the thermopower and completely polarized spin currents.

Firstly, in Chapter 1, we have quiclyk reviewed basic concepts of the Resonant Tunneling Diode (RTD) and the old concept of the Seebeck effect and thermoelectric effects.

Secondly, we have tried to reproduce the results obtained in previous experiments for the RTD with the Landauer-Buttiker formalism. As a result, our model reproduces the physics of our device.

In the Chapter 3, we have studied the thermoelectric effects in the Diode. We have investigated the behaviour of the thermoelectric conductance L. It has a maximum when the Fermi level E_F reaches the energy level of the potential well. However, the Seebeck coefficient does not show the same maximum. For small temperatures we find that the maximum is at the same condition as L. But for higher temperatures the position of the maximum changes linear with temperature. In addition, as we increase the temperature the maximum (in absolute value) changes with temperature approximately as $T^{1/3}$.

The spin effects are considered in the fourth chapter. In our diode a splitting effect is included in the energy of the potential well. This effect involves the conduction of electrons for two different levels (for spin-up or spin-down electrons). We introduce the concept of polarization in the spin current which, in our case, has a maximum (completely polarization) when one of the energy levels has the same value as the Fermi level. The thermoelectric conductance shows an splitting with two maxima at the position of the new levels. Each peak corresponds to a different polarization.

Additionally, we have studied the Seebeck coefficient which now shows two peaks. The two peaks have the same height for small temperatures. But for higher temperatures one peak increases and the other one decreases.

In the Chapter 5 we have introduced a new concept, the Spin Seebeck effect. This effect involves a spin voltage generated by a temperature difference. We have obtained an expression of the spin thermopower for our device. The coefficient is similar as the charge thermopower, but it now shows two peaks with different signs. This result predicts total polarized spin currents originated by a temperature difference.

Much work can still be done in the study of thermoelectric effects in Resonant Tunneling Diodes. A future possible project will be study this system including interactions such as, for example, impurities or interaction among the electrons. Another possible extension will be including multiple barriers in our device (superlattice).

Appendix A

Linearization of the current

As we have seen in the scattering formalism, the electron flow, in general, for the RTD is (eq. 2.9):

$$I = \frac{em^*A}{2\pi^2\hbar^3}\int_{eV}^{\infty} dE_z\ T\left(E_z\right)\int_0^{\infty} dE_\perp[f_{FD_L}\left(E_\perp + E_z\right) - f_{FD_R}\left(E_\perp + E_z\right)] \tag{A.1}$$

First, we will calculate the integral of the Fermi-Dirac distributions. Remember $\mu_L = E_F + eV$ and $\mu_R = E_F$. The f_{FD} are the Fermi-Dirac distributions in each contact and the integrals can be done easily:

$$\int_0^{\infty} dE_\perp\ \frac{1}{1+e^{(E_\perp+E_z-\mu)/k_BT}} = k_BT\ln\left[1+e^{-(E_z-\mu)/k_BT}\right] \tag{A.2}$$

For a temperature difference, the integral of perpendicular energy becomes:

$$T_L\ln\left(1+e^{-(E_z-\mu_L)/k_BT_L}\right) - T_R\ln\left(1+e^{-(E_z-\mu_R)/k_BT_R}\right) \tag{A.3}$$

As a result, the intensity is:

$$I = \frac{em^*A}{2\pi^2\hbar^3}k_B\int_{eV}^{\infty} dE_z\ T\left(E_z\right)\left[T_L\ln\left(1+e^{-(E_z-\mu_L)/k_BT_L}\right) - T_R\ln\left(1+e^{-(E_z-\mu_R)/k_BT_R}\right)\right] \tag{A.4}$$

The temperatures are defined as $T_L = T + \theta_L$ and $T_R = T + \theta_R$, where T is the temperature of the bath and the θ a small applied temperature difference. Therefore, the ter in brackets of the previous expression can be rewritten as:

$$T\ln\frac{1+e^{-(E_z-\mu_L)/k_BT_L}}{1+e^{-(E_z-\mu_R)/k_BT_R}} + \theta_L\ln\left(1+e^{-(E_z-\mu_L)/k_BT_L}\right) - \theta_R\ln\left(1+e^{-(E_z-\mu_R)/k_BT_R}\right) \tag{A.5}$$

It will useful to make a linearization of the previous expression. It is a function of the form $f(V,\theta_L,\theta_R)$. Then, the linearization is:

$$f(V,\theta_L,\theta_R) = f(0,0,0) + eV\left.\frac{\partial f}{\partial V}\right|_{\theta_L=\theta_R=V=0} + \theta_L\left.\frac{\partial f}{\partial\theta_L}\right|_{\ldots 0} + \theta_R\left.\frac{\partial f}{\partial\theta_R}\right|_{\ldots 0} \tag{A.6}$$

The derivative on V is:

$$\frac{\partial f}{\partial V} = eT\frac{\frac{1}{k_BT_L}\ e^{-(E_z-E_F-eV)/k_BT_L}}{1+e^{-(E_z-E_F-eV)/k_BT_L}} + e\theta_L\left(\frac{\frac{1}{k_BT_L}\ e^{-(E_z-E_F-eV)/k_BT_L}}{1+e^{-(E_z-E_F-eV)/k_BT_L}}\right) \tag{A.7}$$

Using the conditions of the linearization:

$$\left.\frac{\partial f}{\partial V}\right|_{\ldots 0} = \frac{e}{k_B}\ \frac{1}{1+e^{(E_z-E_F)/k_BT}} = \frac{e}{k_B}\ f_{FD}\left(E_z\right) \tag{A.8}$$

The derivative for θ_L is:

$$\frac{\partial f}{\partial \theta_L} = T\frac{e^{-(E_z-E_F-eV)/k_BT_L}\left(\frac{E_z-E_F-eV}{k_BT_L^2}\right)}{1+e^{-(E_z-E_F-eV)/k_BT_L}} + \ln\left(1+e^{-(E_z-E_F-eV)/k_BT_L}\right) + \theta_L\frac{e^{-(E_z-E_F-eV)/k_BT_L}\left(\frac{E_z-E_F-eV}{k_BT_L^2}\right)}{1+e^{-(E_z-E_F-eV)/k_BT_L}} \tag{A.9}$$

With the condition we obtain:

$$\frac{\partial f}{\partial \theta_L} = \frac{E_z - E_F}{k_BT}\ \frac{1}{1+e^{(E_z-E_F)/k_BT}} + \ln\left(1+e^{-(E_z-E_F)/k_BT}\right) \tag{A.10}$$

Similarly, the case of the derivative of θ_R gives the same result as before but with a global negative sign. Consequently, the intensity can be written as:

$$I = \frac{em^*A}{2\pi^2\hbar^3}\int_{eV}^{\infty} dE_z\ T\left(E_z\right) \times \left(\frac{1}{k_B} f_{FD}\left(E_z\right) eV \right. \\ \left. + \left(\theta_L - \theta_R\right)\left[\frac{E_z - E_F}{k_BT}\ f_{FD}\left(E_z\right) + \ln\left(1+e^{-(E_z-E_F)/k_BT}\right)\right]\right) \tag{A.11}$$

Appendix B

Calculation of the Spin Seebeck effect

Since we have two energy levels for each spin, we have two contributions to the total current, one for the spin-up electrons and one for spin-down electrons. That can be written in the form of equation 3.2:

$$I_{\uparrow} = \frac{em^*A}{4\pi^2\hbar^3}k_B \int dE_z \; \frac{\Gamma_L\Gamma_R}{(E-E_{0\uparrow})^2 + \left(\frac{\Gamma_L+\Gamma_R}{2}\right)^2} \left[T_L \ln\left(1+e^{-(E_z-\mu_L)/k_BT_L}\right) - T_R \ln\left(1+e^{-(E_z-\mu_R)/k_BT_R}\right)\right] \tag{B.1}$$

$$I_{\downarrow} = \frac{em^*A}{4\pi^2\hbar^3}k_B \int dE_z \; \frac{\Gamma_L\Gamma_R}{(E-E_{0\downarrow})^2 + \left(\frac{\Gamma_L+\Gamma_R}{2}\right)^2} \left[T_L \ln\left(1+e^{-(E_z-\mu_L)/k_BT_L}\right) - T_R \ln\left(1+e^{-(E_z-\mu_R)/k_BT_R}\right)\right] \tag{B.2}$$

As in the appendix A, we want to linearize the terms in brackets. But now, we derive as a function of the electrochemical potentials. Notice that they differ in the electrochemical potentials μ. For instance, for the spin up current we have:

$$[\ldots] \longrightarrow f(\theta_L, \theta_R, \mu_{L\uparrow}, \mu_{R\uparrow}) \tag{B.3}$$

Therefore, the derivatives of each parameter are:

$$\begin{array}{lcl} \left.\frac{\partial f}{\partial \theta_R}\right|_{\substack{\theta_L=\theta_R=0 \\ \mu_{L\uparrow}=\mu_{R\uparrow}=E_F}} & = & \frac{E_z-E_F}{k_BT}\;\frac{1}{1+e^{(E_z-E_F)/k_BT}} + \ln\left(1+e^{-(E_z-E_F)/k_BT}\right) \\ \left.\frac{\partial f}{\partial \theta_L}\right|_{\ldots} & = & -\left.\frac{\partial f}{\partial \theta_R}\right|_{\ldots} \\ \left.\frac{\partial f}{\partial \mu_{L\uparrow}}\right|_{\ldots} & = & \frac{1}{k_B}\frac{1}{1+e^{(E_z-E_F)/k_BT}} \\ \left.\frac{\partial f}{\partial \mu_{R\uparrow}}\right|_{\ldots} & = & -\left.\frac{\partial f}{\partial \mu_{L\uparrow}}\right|_{\ldots} \end{array} \tag{B.4}$$

For the current corresponding to spin-down electrons the solution is exactly the same but with up arrows. Hence, the linearized carrier flows are:

$$I_{\uparrow} = \frac{em^*A}{4\pi^2\hbar^3}k_B \int dE_z \; \frac{\Gamma_L\Gamma_R}{(E-E_{0\uparrow})^2 + \left(\frac{\Gamma_L+\Gamma_R}{2}\right)^2} \left\{\left[\frac{E_z-E_F}{k_BT}\;\frac{1}{1+e^{(E_z-E_F)/k_BT}} + \ln\left(1+e^{-(E_z-E_F)/k_BT}\right)\right]\Delta T + \left[\frac{1}{k_B}\frac{1}{1+e^{(E_z-E_F)/k_BT}}\right](\mu_{L\uparrow}-\mu_{R\uparrow})\right\} \tag{B.5}$$

$$I_\downarrow = \frac{em^*A}{4\pi^2\hbar^3}k_B\int dE_z\,\frac{\Gamma_L\Gamma_R}{(E-E_{0\downarrow})^2+\left(\frac{\Gamma_L+\Gamma_R}{2}\right)^2}\left\{\left[\frac{E_z-E_F}{k_BT}\,\frac{1}{1+e^{(E_z-E_F)/k_BT}}+\ln\left(1+e^{-(E_z-E_F)/k_BT}\right)\right]\Delta T\right.$$
$$\left.+\left[\frac{1}{k_B}\frac{1}{1+e^{(E_z-E_F)/k_BT}}\right](\mu_{L\downarrow}-\mu_{R\downarrow})\right\} \quad \text{(B.6)}$$

We can redefine these expressions as:

$$\begin{array}{rcl} I_\uparrow &=& L_\uparrow\Delta T + G_\uparrow(\mu_{L\uparrow}-\mu_{R\uparrow}) \\ I_\downarrow &=& L_\downarrow\Delta T + G_\downarrow(\mu_{L\downarrow}-\mu_{R\downarrow}) \end{array} \quad \text{(B.7)}$$

in terms of the electric conductance and thermoelectric conductance G and L respectively. Note that are they are the same transport coefficients as in the section where we study the magnetic RTD. These coefficients take into account the effects of spin.

Recalling that the voltage is the difference of electrochemical potentials of two leads and the definitions from eq. 5.2 and 5.3:

$$\begin{array}{rcl} eV &=& \mu_L-\mu_R \\ \mu_\alpha &=& \frac{1}{2}(\mu_{\alpha\uparrow}+\mu_{\alpha\downarrow}) \\ eV_S &=& (\mu_{L\uparrow}+\mu_{L\downarrow})-(\mu_{R\uparrow}+\mu_{R\downarrow}) \end{array} \quad \text{(B.8)}$$

we can write the charge current as:

$$I = I_\uparrow + I_\downarrow = (L_\uparrow+L_\downarrow)\Delta T + (G_\uparrow+G_\downarrow)eV + \frac{1}{2}(G_\uparrow-G_\downarrow)eV_S \quad \text{(B.9)}$$

And the spin current is:

$$I_S = I_\uparrow - I_\downarrow = (L_\uparrow-L_\downarrow)\Delta T + (G_\uparrow-G_\downarrow)eV + \frac{1}{2}(G_\uparrow+G_\downarrow)eV_S \quad \text{(B.10)}$$

Bibliography

[1] G.E. Moore. *Cramming more components onto integrated circuits.* Proceedings of the IEEE. **86**, 82 (1998)

[2] A.Fert and P.Grunberg. *Better read-out heads for pocket-size devices.* Nobel Lecture. 2007

[3] L.Esaki. *Long journey into Tunneling.* Nobel lecture. 1973

[4] L.L.Chang, L.Esaki, R.Tsu. *Resonant Tunneling in semiconductor barriers.* Appl. Phys. Lett. **24**, 593 (1974)

[5] L.Esaki. *New Phenomenon in Narrow Germanium $p-n$ Junctions.* Physical Review. **109**, 603 (1958)

[6] F.Capasso, S.Datta. *Quantum electron devices.* Physics Today. **43**, 74 (1990)

[7] K.Ikoma, M.Munekiyo, K.Furuya, M.Kobayashi, T.Izumi, and K.Shinohara. *Thermoelectric module and generator for gasoline engine vehicles.* IEEE 17th International conference on Thermoelectrics. 464 (1998)

[8] D.Kramer *Shortage of Plutonium-238 Jeopardizes NASA's Planetary Science Missions.* Physics Today. **64**, 24 (2011)

[9] G.D.Mahan and J.O.Sofo. *The best thermoelectric.* PNAS. **93**, 7436 (1995)

[10] G.J.Snyder and E.S. Toberer. *Complex thermoelectric materials.* Nature. **7**, 105 (2008)

[11] R.Venkatasubramanian, E.Siivola, T.Colpitts and B.O'Quinn. *Thin-film thermoelectric devices with high room-temperature figures of merit* Nature. **413**, 597 (2001)

[12] L.D.Hicks, M.S. Dresselhaus. *Effect of Quantum-well structures on the thermoelectric figure of merit.* Physical Review B. **47**, 12727 (1993)

[13] T.C.Harman, P.J.Taylor, M.P.Walsh and B.E.Laforge. *Quantum dot superlattice thermoelectric materials and devices.* Science. **297**, 2229 (2002)

[14] R.Kim, S.Datta and M.S.Lundstrom. *Influence of dimensionality in thermoelectric device performance.* Journal of Applied Physics. **105**, 034506 (2009)

[15] L.D.Hicks and M.S.Dresselhaus. *Thermoelectric figure of merit of one-dimensional conductor.* Physical Review B. **47**, 16631 (1993)

[16] S. Datta. *Electronic transport in mesoscopic systems.* Cambridge University Press. 1995

[17] M.Buttiker, Y.Imry, R.Landauer, S.Pinhas *Generalized many-channel conductance formula with applications to small rings.* Physical review B. **31**, 6207 (1985)

[18] D.D.Coon, K.M.S.V. Bandara and H.Zhao. *Breit-Wigner description of resonant tunneling.* Applied Physics Letters. **55**, 2453 (1989)

[19] R.Tsu, L.Esaki. *Tunneling in a finite superlattice.* Applied Physics Letters. **22**, 562 (1973)

[20] A.Slobodskyy, C. Gould, T.Slobodsky, G. Schmidt, L.W. Molenkamp and D. Sánchez. *Resonant tunneling diode with spin polarized injector.* Applied Physics Letters. **90**, 122109 (2007)

[21] J.A.Gaj, R. Planel, and G. Fishman. Solid State communications. **29**, 435 (1979)

[22] R.Scheibner, H.Buhmann, D.Reuter, M.N.Kiselev and L.W.Molenkamp *Thermopower of a Kondo Spin-Correlated Quantum Dot.* Physical Review Letters. **95**, 176602 (2005)

[23] A.Slobodskyy, C. Gould, T.Slobodsky, C.R. Becker, G. Schmidt, and L.W. Molenkamp. *Voltage-Controlled Spin Selection in a Magnetic Resonant Tunneling Diode.* Physical Review Letters. 90, 2466011 (2003)

[24] W.Pacuski, D.Ferrand, J.Cibert, J.A.Gaj, A. Golnik, P.Kossacki, S.Marcet, E.Sarigiannidou and H.Mariette. *Excitonic gian Zeeman effect in GaN:Mn^{3+}.* Physical Review B. **76**, 165304 (2007)

[25] A.Slobodskyy. *Diluted magnetic semiconductors Resonant Tunneling structures for spin manipulation.* PhD thesis. Univeristy of Wurzburg. 2005

[26] I.Zutic, J.Fabian and S.Das Sarma. *Spintronics: Fundamentals and applications.* Reviews of Modern Physics. **74**, 323 (2004)

[27] T.Rejec, R.Zitko, J.Mravlje and A.Ramsak. *Spin thermopower in interacting quantum dots.* Physical Review B. **85**, 085117 (2012)

[28] K.Uchida, S.Takahashi, K.Harii, J.Ieda, W.Koshibae, K.Ando, S.Maekawa and E.Saitoh. *Observation of the spin Seebeck effect.* Nature. **455**, 778 (2008)